PERGAMON

Carbon 41 (2003) 797–809

CARBON

Characterization of multiwall carbon nanotubes and influence of surfactant in the nanocomposite processing

S. Cui[a,1], R. Canet[a], A. Derre[a], M. Couzi[b], P. Delhaes[a,*]

[a]*Centre de Recherche Paul Pascal CNRS and Université Bordeaux I, No. 115 Avenue Albert Schweitzer, 33600 Pessac, France*
[b]*Laboratoire de Physico-Chimie Moléculaire—Université Bordeaux I, 351 cours de la Libération, 33405 Talence Cedex, France*

Received 19 August 2002; accepted 16 November 2002

Abstract

Carbon nanotubes prepared by a classical CVD method with a nickel catalyst have been characterized, then used as conducting anisometric objects dispersed into a polymeric matrix. In a first part, these nanotubes are structurally characterized before and after heat treatments (HTT=1500, 2000, 2500 °C). Diffusion Raman experiments and diamagnetic susceptibility experiments demonstrated their limited graphitized structures.Then, in a second step, a well defined processing way to prepare nanocomposites with a standard epoxy resin is presented. In particular, the use or not of a non-ionic surfactant (Tergitol) to disperse these nanotubes is analyzed. The influence of nanotube contents is examined on the bulk nanocomposite density, the glass transition temperature of the nanocomposites, and the d.c. electrical conductivity behavior. These results demonstrated that the interfacial properties are playing a fundamental role. On one hand, the glass transition temperature is increasing with the nanotube content, and on the other hand, the percolation threshold is found for a rather high critical volumic concentration. Finally, it is demonstrated that a pure geometrical model is not sufficient to explain these behaviors and that a wrapping effect of the organic matrix around the nanotubes has to be considered.

Keywords: A. Carbon nanotubes; C. Raman spectroscopy; D. Electrical properties; Magnetic properties

1. Introduction

Solid carbons are known for exhibiting different polymorphic forms associated with the different types of hybridization bondings which are occuring in atomic carbons. These different chemical bondings leads to the diamond, graphite and carbyne type structures. One step further has been realized with the recent discoveries of curved graphene sheets namely the fullerenes and nanotubes [1].

In particular, the synthesis of hollow nanotubes consisting of concentric cylindrical atomic sheets, single wall and multiwall nanotubes (SWNT, MWNT) have given a large impetuosity in the nanotechnology developments [2]. One particular research direction, which is concerned by this study, is about nanocomposites on which several researches have been carried out these last years. Most of the works are devoted to design advanced polymeric nanocomposites which should present improved properties either conducting or mechanical because the carbon nanotubes are considered as the ultimate carbon fibers [3].

It turns out that these nanocomposites are dependent of both the component choice and the selected processing way. We can examine briefly what are these main factors.

1.1. Nanotubes and nanofilaments

The nanotubes, mainly MWNT, belong to a large family of filamentary carbons which are known for a long time as vapor grown carbon fibers (VGCF). Depending upon the experimental conditions based on catalytic cracking of hydrocarbon gases, standard fibers of micrometric diameter [4] submicronic [5] or even nanometric size [6] have been produced.

Their structural characteristics are related with their diameter (D) which can vary over four orders of magnitude, and the so-called aspect ratio L/D, where L is the

*Corresponding author. Tel.: +33-556-84-5694; fax: +33-556-84-5600.
E-mail address: delhaes@crpp.u-bordeaux.fr (P. Delhaes).
[1]Visiting Professor from Tianjin University, China.

0008-6223/02/$ – see front matter
doi:10.1016/S0008-6223(02)00405-0

mean length of each filament, which is very large, typically $L/D \approx 10^2-10^3$. This geometrical factor leads to a very low percolation threshold, i.e., a conducting charged polymer for a very low concentration of these fillers [7]. Moreover the different morphological characteristics of carbon layers based on the geometrical arrangement of the basic structural units (BSU) is fundamental. In standard nanotubes the aromatic layers are concentric along the tube axis whereas in other cases a bamboo shape or a fishbone morphology with an ill-defined central canal is observed by transmission electronic microscopy (TEM) [8]. These nanostructures are fundamental for the interfacial contacts both in size (available specific area) and in nature (hydrophobic character of an ideal graphene surface, presence of active sites and edge states of BSU defects) [9]

1.2. Polymeric matrices and processing

Many polymers belonging to the thermoplastic or the thermoset class have been widely investigated [7]. The choice conditioning the type of process is imposed by the homogeneous dispersion of the filler inside the matrix; this requirement implies a surface treatment, the use of a surfactant and the choice of mixing process as a shear technique or some alignment way to enhance the mechanical properties in one given direction [10].

In particular, to improve the wetting action and the dispersion stability of nanotubes different surfactants have been proposed. They are ionic surfactants as sodium dodecyl sulfate (SDS) [11] which can be used with hydrosoluble polymers as for example polyvinylalcohol (PVA) or polycarbonates. Alternatively non-ionic surfactants have been proposed when organic solvents have to be used as for epoxy resins [12].

It is interesting to note that a surface treatment of nanotube, implying a surface functionalization and grafted polymer is very interesting but not yet plainly developed for making these multiphase materials [13]. The major point to underline is the role of the interfacial adhesion for electrical or for load transfer governing the interfacial shear stress. They depend both on the polymer characteristics as the glass transition, and the nature of the carbon surface, but also of the surfactant presence. This is well known for example in the case of carbon black particles which form composite materials exhibiting different critical volumic fractions related to the percolation thresholds and sensitive to the involved polymer [14].

This remark is also relevant for nanocomposites using either single wall or multiwall nanotubes with different polymers; from the literature it is observed that the critical volumic fractions are scanning between 1 and 10% without any clear relationship between filler and matrix.

It turns out that to prepare nanocomposites with improved physical properties it is necessary to control together the components and the processing way. In this work, we have firstly developed the physical and structural characterizations of catalytically grown nanotubes [15]. Then, in a second part, we present a mixing process based on the nanotube dispersion using a non-ionic surfactant (Tergitol NP 7) associated with ultrasonic and shearing techniques using a classical epoxy resin. We have characterized two series of nanocomposites, with and without surfactant, using helium pycnometry for density determination, glass transition measurement using differential scanning calorimetry (DSC) and d.c. electrical resistivity experiments.

2. Nanotube and nanofilament characterizations

Since their discovery by IIJIMA [16], the single wall carbon nanotubes have attracted a large interest, but the main challenge remains their reproducible production and purification before any use. Basically, two main classes of techniques have been developed for SWNT and MWNT growths, which are, respectively, the physical methods based on graphite vaporization at high temperature and the catalytic thermal decomposition of hydrocarbons [2].

The chemical vapor deposition (CVD) method [6] which involves the use of catalyst as Fe, Co, Ni at moderate temperatures (below 1000 °C) is a very attractive method in particular for MWNT [17]. The main advantages are a low cost synthesis associated with a large scale production. Nevertheless some disadvantages are also present even with a careful control of the CVD parameters. They are mainly related to the impurities, the formation of amorphous carbon particles and the remaining catalytic nanoparticles even if efforts are carried out to lower the catalyst amount. The subsequent purification techniques are therefore crucial to obtain a homogeneous batch [18].

It turns out that both the morphology and the physical properties of these MWNT are dependent of the production technique and a full characterization is necessary before using them as a conductive filler in a polymeric matrix. We have, therefore, carefully examined the structural and morphological changes of these nanofibers under further graphitation heat treatments which are compared to the as grown ones at 600 °C.

Then, we have studied some physical properties, as magnetic susceptibility and Raman spectroscopy to get a deeper insight on these nanotubes.

2.1. Nanotubes preparation

As already described [15], these multiwall nanotubes are prepared by CVD of methane at 600 °C in presence of a nickel catalyst. The yield obtained after several hours is around 20–30% and several grams can be prepared during one run. By purification using nitric acid 2 M at 60 °C during 4 h and a careful washing, a batch of purified MWNT is obtained. TEM photographs show the presence of nickel nanoparticles inside the nanotubes which present

usually as a worm like tube with an inner diameter of a few nanometers and an outside one ranging from 10 to 50 nm (see next part).

On this purified batch which does not contain almost any soot type particle a series of heat-treatment temperature (HTT) has been pursued thanks to a standard graphite furnace. In order to examine the graphitation process heat-treatments under neutral atmosphere at respectively 1500, 2000 and 2500 °C during 1 h and half have been done; respective weight losses of 2.5% at 1500 °C and 3.2% at 2000 and 2500 °C have been measured.

On these different batches a surface analysis, using standard photoelectron spectroscopy with a X-ray beam on a small surface area, has allowed us to detect the presence of inorganic impurities and surface functionalities [19].

The XPS survey on the purified batch shows several absorption peaks a strong one corresponding to the carbon peak 1*s* (286 eV) and mainly two quite small ones attributed to oxygen 1*s* (531 eV) and Nickel 2*p* (854 eV) which do not change significantly after etching. For the heat-treated samples the presence of a nickel compound is almost disappearing but a very small amount of oxygene is still present. A more detailed XPS spectra relative to the *C*(1*s*) line is given in Fig. 1 for the different samples. We observe immediately a larger peak at 284.2 eV for the pristine sample than for the other samples which present a «sp^2-like» carbon peak as in graphite. It seems that for the initial sample C–O or C=O, bondings which are located at a higher energy, are present but they disappear after thermal annealing under an inert atmosphere [19].

2.2. Structural and morphological analysis

The nanotube morphology is analyzed by transmission electron microscopy (JEOL JEM 2000 FX); as usual the TEM micrographs are recorded on dilute suspensions dried on a carbon film coated on a copper grid. Aggregates of vermicular objects with a width around 50 nm and a length of several micrometers are observed as previously [15]. In Fig. 2 we give two examples of these nanotubes one as purified (a) and after heat-treatment (b); the graphitic BSU planes form a definite angle with the tube axis giving a kind of «herring-bone» structure with an open channel [3]. By comparison between these photographs we observe that the graphitation, i.e., the long range ordering of BSU is not very efficient; nevertheless, the catalytic nickel type nanoparticles are disappearing after this heat-treatment.

These observations are confirmed by X-ray diffraction experiments (INEL diffractometer) and pycnometry (Accupyc 130-Micromeritics). The experimental values, mean interlayer spacing d_{002} (Å) and intrinsic density, respectively, are reported in Table 1. We observe firstly that the initial nanotube density is higher than after thermal treatment: this is due to the residual presence of catalyst as already observed. Secondly, the mean distance between graphitic planes is rather large and weakly dependent of any further treatment indicating that a full graphitation process is not occuring. With this morphology the aromatic layers cannot be extended at the opposite of the regular nanotubes which present concentric graphene layers [5,8].

2.3. Physical properties

To characterize these nanotubes we used two relevant electronic properties which are respectively the magnetic susceptibility and the Raman spectroscopy.

The magnetic susceptibility has been measured between 2 and 300 K with a SQUID magnetometer (Quantum design MPMS-5) under a magnetic field strength of 10 K gauss. The nanotubes are randomly dispersed inside a capsule and we measure a mean magnetization and we determine a mean susceptibility value $\langle\chi\rangle$ (emu g^{-1}). Both on the purified sample and after heat-treatment at 1500 °C we determine a paramagnetic susceptibility (the room temperature values are respectively around $+1.6\ 10^{-5}$ and

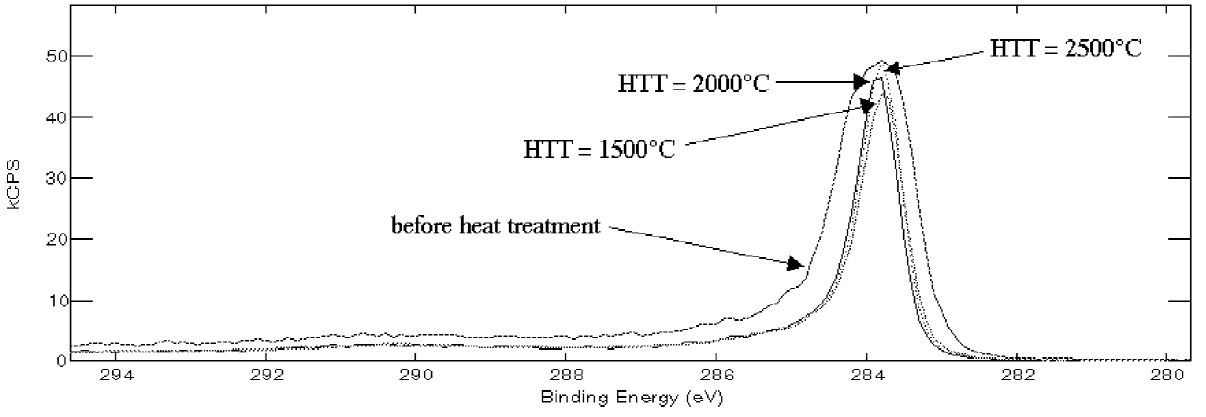

Fig. 1. XPS spectra recorded at room temperature on C(1*s*) atoms on the series of nanotubes, before and after heat-treatments (HTT).

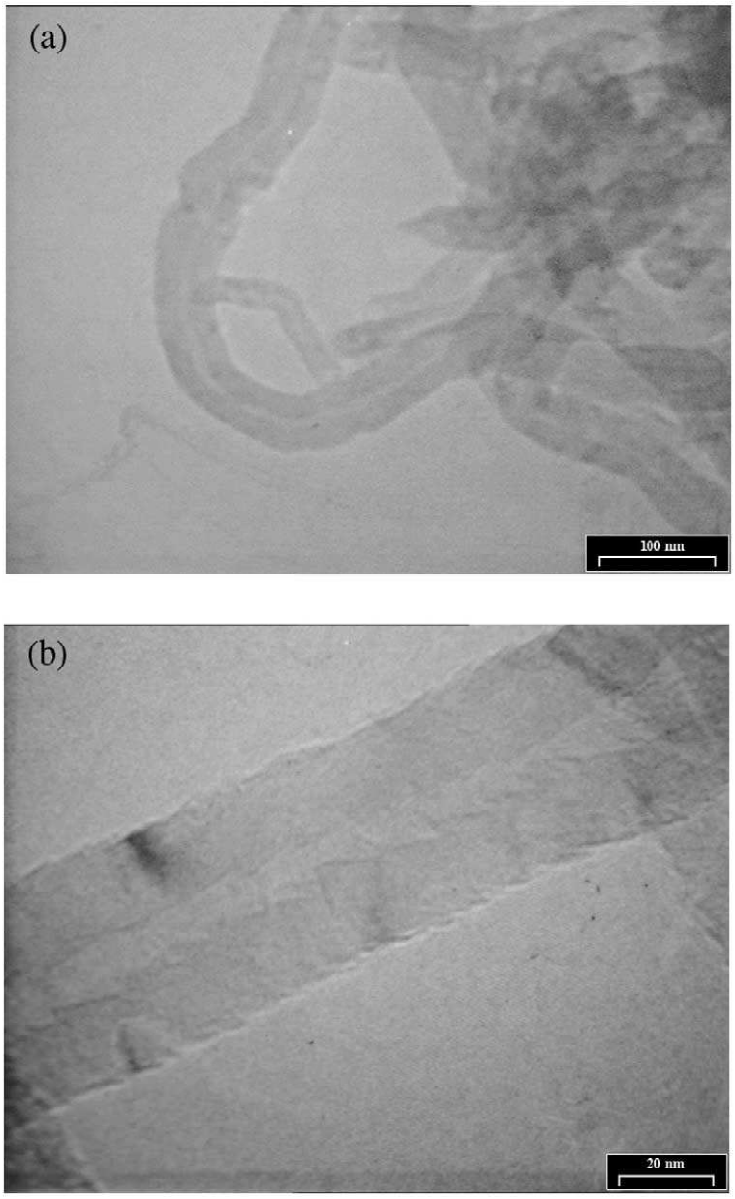

Fig. 2. High resolution TEM micrographs of nanotubes (a) purified batch (b) after treatment at HTT = 2000 °C.

Table 1
Structural characteristics of the investigated MWNT

Samples	Density (He pycnomety)	Interlayer spacing d_{002} (Å)	Crystallite size L_a (Å)
Purified MWNT	2.25 ± 0.02	3.482 ± 0.02	≈30*
HTT = 1500 °C	2.08	3.468	
HTT = 2000 °C	2.11	3.480	60 +
HTT = 2500 °C	2.09	3.462	80 +

*L_a value estimated from TEM observations, + L_a values deduced from diamagnetism experiments.

1.0 10^{-5} emu g^{-1}). These results are indicating the presence of paramagnetic nickel compounds inside the nanotubes. After higher heat treatments, we observe, however, a different situation with the occurrence of a bulk diamagnetic susceptibility with a small low temperature Curie tail (Fig. 3). This observation is related to the vaporization of inorganic impurities at high temperatures. As well known for graphitic carbons [20] and more recently for nanotubes [21,22], the presence of a Landau diamagnetism is characteristic of a two-dimensional π-type electron system known for a long time. This diamagnetism is related to the surface of π delocalization which is constitued by the polyaromatic BSU and characterized by a so-called crystallite size L_a (Å). From the observed room temperature values which are situated at intermediate values between aromatic compounds ($\chi = -0.8\ 10^{-6}$ emu g^{-1}) and polycristalline graphite ($\chi = -6.5\ 10^{-6}$ emu g^{-1}) we can estimate this parameter from an experimental curve established for classical graphitic carbons [20]. We deduce immediately that $L_a \approx 60$ and 80 Å after HTT = 2000 and 2500 °C, respectively. This result indicates a weak graphitation process in agreement with X-ray diffraction results on d_{002} spacings (see Table 1).

Raman spectroscopy has been used extensively as a surface characterization technique for carbon materials and more recently for nanotubes [23]. The spectra were collected in back-scattering geometry, using a LABRAM spectrometer by DILOR with a CDD detector. The sample was excited by the 632.8 nm of a He–Ne laser. A confocal microscope equipped with a 100× magnification objective was used both to focus the laser beam on the sample and to collect the scattered light. The laser spot on the sample was around 1 μm^2 with an incident power of about 1 mW. The Raman active modes in nanotubes are classical tangential modes and radial ones of curved graphene sheets. Currently we are only interested by the tangential modes which are based on the first order Raman spectra of ideal graphite with a characteristic single peak at 1580 cm^{-1} (G-band) which corresponds to one of the two Raman active E_2g vibrations of hexagonal graphite structure. But the ability of this spectroscopy is to detect any structural disorder with the presence of additional bands located around 1350 cm^{-1} (D-band) and 1620 cm^{-1} (D'-band which appears as a shoulder on the G-band). Second order lines are also detected at about 2600 cm^{-1} (G'-band) which can become a doublet in presence of a c-axis ordering after graphitation [23].

All these bands with their respective characteristics, intensity, position and width are relevant parameters for characterising the different structural disorders [24]. The most useful approach has been proposed by TUINSTRA and KOENIG [25] who have noted that the integrated intensity ratio of the D band (breathing mode A_{1g}) to G band is varying inversely with L_a (for $L_a > 20$ Å):

$$R(\lambda) = \frac{I(D)}{I(G)} = \frac{C(\lambda)}{L_a} \quad (1)$$

$C(\lambda)$ is a variable scaling coefficient depending on the excitation wavelength λ, because the D-band is associated with a resonance effect due to the π electronic gas:

$$C(\lambda) = C_0 + \lambda C_1 \quad (2)$$

With $C_0 = -126$ Å and $C_1 = 0.033$ [26].

Fig. 4 shows the Raman spectra of the different batches before and after heat treatment; they all exhibit similar features with the four resolved bands D, G, D' and G' situated at the expected positions. The most striking spectral evolution concerns the intensity ratio $I(D)/I(G)$ as defined in Eq. (1) which is decreasing with increasing HTT. Furthermore, we evaluated L_a from TEM photo-

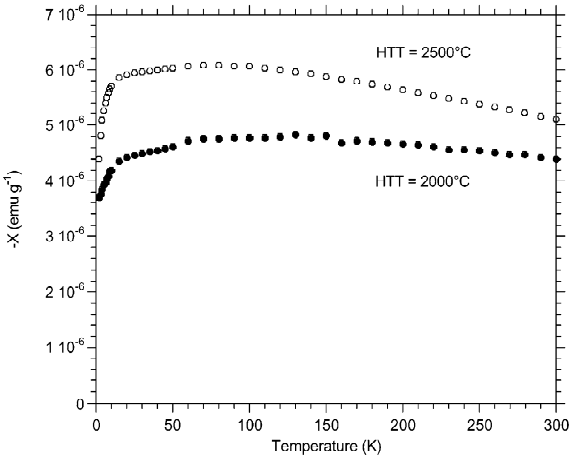

Fig. 3. Static diamagnetic susceptibility versus temperature for the nanotube batches heat-treated at 2000 and 2500 °C, respectively.

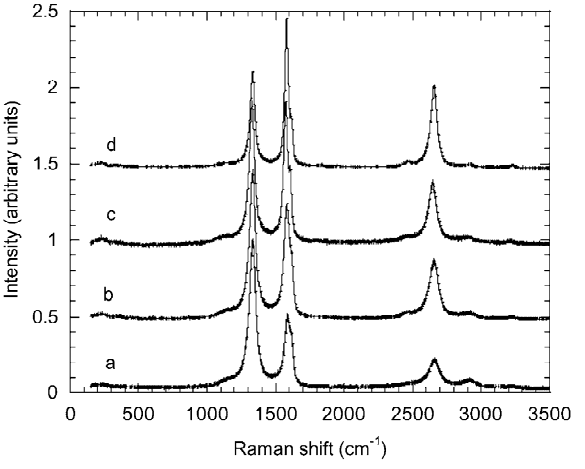

Fig. 4. Raman spectra of the different batches (a) as grown after purification (b, c and d) after heat-treatments at 1500, 2000 and 2500 °C, respectively.

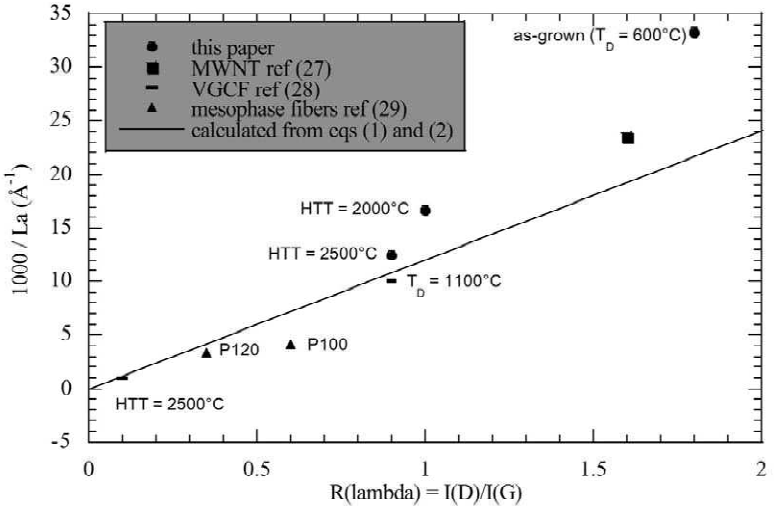

Fig. 5. Relation between the intensity ratio $R(\lambda) = I(D)/I(G)$ (measured for $\lambda = 632.8$ nm) and the mean crystallite size (L_a); the straight line is obtained from Eqs. (1) and (2).

graphs and magnetic measurements, so that we are able to test the validity of relations (1) and (2), as plotted in Fig. 5 for $C(\lambda) = 82.8$ Å [26]. For comparison, we have reported the available results obtained in this study and according to different sources [27–29]. The general empirical relationship described by Eqs. (1) and (2) is roughly obeyed for this family of filamentous carbons with different diameters ranging from 30 nm to 10 μm. Indeed, the ratio $R(\lambda)$ is an indicator of the mean size of π electron delocalized systems which are related to the electrical conductivity on the one hand and to the elastic modulus on the other hand; so, these physical quantities increase when $R(\lambda)$ decreases, i.e., when a more graphitized state is reached. At the opposite of well graphitized nanotubes or filaments, we confirm here that this type of «herring bone» distribution of graphitic planes cannot produce a well graphitized structure. It turns out that their bulk physical properties are not optimized with surface characteristics which are not those of ideal graphene, i.e., low energy surface with an hydrophobic character.

3. Nanocomposites: process and characterization

3.1. Strategy and experimental way

As it has been presented in the general introduction, the nanocomposites are dependent of the constituents but also of the processing way because of the large increase of the nanotubes or nanofiber surface area at a given volumic fraction of filler; their dispersion is a key parameter. The use of both a surfactant and a solvant is crucial to disperse the nanotubes, but it has to be associated with a careful processing technique. These parameters are dependent with the matrix choice which will be a classical thermoset polymer. The epoxy resin Araldite D from Ciba-Geigy (diglycidyle ether of bisphenol) is mixed with an amine type hardener (HY 956) under the ratio 10:2 in weight. In such a case, it is necessary to use a non-ionic surfactant which will be Tergitol NP 7 which is a Nonylphenyl ether (from Union Carbide-Sigma) in presence of a selected light solvant (acetone).

Our process, which is derived from previous works with epoxy resins [30,31], is based on three steps:

(i) Dispersion of nanotubes: after a light grinding in a mortar to disperse the main bundles, the MWNT are dispersed in pure acetone or acetone solution with Tergitol (2% weight) in a glass tube. This mixture is kept for 30 min inside a strong ultrasonic bath cooled with ice. This dispersion process is checked by optical microscopy observations to proof its efficiency [11].

(ii) Mixing of resin: The araldite D is added to the dispersed solution of nanotubes then dispersed again in the ultrasonic bath during 15 min. Then the mixture is mixed for 1 h, at 80 °C for decreasing its viscosity, by shear mixing with a rotating blade. The solution is placed under vaccum and the same experimental set-up to evaporate completely the solvant (1 h). Finally the mixture is cooled down to room temperature.

(iii) Polymerization: The polymerizing agent is added then mixed to this above mixture which is introduced in a molder. This stirring solution is polymerized at 120 °C during 1 h then slow cooled down to room temperature to prevent any thermal stress. The final sample ($\phi = 12$ mm, $h = 30$ mm) is removed from its container then cut with a diamond saw at the proper shape for one given experiment.

Following this process, we have investigated two sets of parameters:

- Influences of solvant and surfactant and its used amount to cover the nanotube surface.
- Graphitation effect by comparison between the as grown and purified batch and after heat-treatment at 2000 °C when all the catalyst particles are eliminated.

To examine their influences we have systematically measured the following properties:

- The intrinsic density by He pycnometry which allows us to determine the effective nanocomposite density and to check the absence of sizable closed porosity.
- The glass transition temperature of the epoxy resin ($T_g \approx 40$ °C) which is sensitive to interfacial interactions in some cases [32]. This characteristic temperature which reveals the motion of polymer chains and a sharp decrease of the viscosity, is determined by differential scanning calorimetry (Perkin-Elmer, Pyris 1 model). For these experiments we have used a rate temperature of 5 °C per minute raising between 20 and 80 °C; from the determined enthalpic change we determine Tg and the associated transition width (ΔT_g) thanks to the standard tangential method.
- The d.c. electrical conductivity using silver paste for a classical four points or a two points method for insulating samples (Electrometer KEITHLEY 617). This technique is appropriate to examine the presence or not of conducting aggregates inside the matrix.

3.2. Description and analysis of results

3.2.1. Preliminary studies

With the purpose to clarify the role of the main parameters and to establish the described process we have carried out different series of experiments. Firstly, as reported in Table 2, we have examined the respective role of nanotubes (before and after heat-treatment) and of additives (surfactant and solvant) in the epoxy resin. Secondly, we have specifically investigated the influence of Tergitol content to homogeneously disperse these nanotubes; to optimize the experimental conditions, observations by optical microscopy have been done, as already described [11], to detect the formation of aggregates in the suspension.

The main information drawn from Table 2 are the following:

- The plain epoxy resin is not strongly modified by acetone if the solvant is completely extracted. Besides the selected polymerisation time (1 h) is enough; further duration does not change significantly the polymer characteristic in particular the glass transition temperature.
- The introduction of a small amount of nanotubes (0.26% in weight) is accompanied by a small increase of the bulk density with a small decrease of the electrical resistivity (about one order of magnitude). However, no significant difference is observed between the two batches; this point is confirmed by the weak graphitation ability that we already observed (see Table 1).

Table 2
Physical properties of different series of nanocomposites

Nanocomposites	Physical properties			
Nanotubes and additives in epoxy matrix	Density	T_g and ΔT_g (°C)		Electrical resistivity (ohm.cm)
No MWNT				
No	1.17	43.9	35	$5.0\ 10^{12}$
Acetone	1.18	40.2	32	$4.3\ 10^{12}$
Acetone + Tergitol (2%)	1.17	39.7	35	$2.5\ 10^{12}$
As purified (0.26% in weight)				
Acetone	1.19	46	40	$1.0\ 10^{11}$
Acetone + Tergitol (2%)	1.18	42	40	$2.5\ 10^{11}$
After heat treatment HTT = 2000 °C (0.26% in weight)				
No	1.19	44	38	$1.0\ 10^{11}$
Acetone + Tergitol (2%)	1.19	42	40	$0.8\ 10^{11}$

As we have pointed out in the Introduction, a large interface is the fundamental characteristics for all these nanocomposites. In order to obtain metastable nanotube suspension, we have evaluated the necessary amount of Tergitol. Assuming a cylindrical shape and considering the external surface only, we estimated the available surface at least around 50 $m^2\ g^{-1}$ value, which is not so far from the specific surfaces obtained from BET experiments on similar MWNT [9].

After assuming that each surfactant molecule will interact mainly with its alkyl side the interactive area will be around 0.4 nm^2. If we want to introduce up to 10% in weight of nanotubes inside the polymer, around 1–2% in weight of surfactant is necessary to fully saturate the carbon surface by physical adsorption. We have therefore examined the influence of tergitol amount on the dispersion quality and the resulting physical properties. In the case of 0.26% in weight of nanotubes, a good dispersion and a grey homogenous image is observed by optical microscopy as already shown [11]. However, when we increase the MWNT concentration the presence of small clusters is randomly detected. The influence of tergitol amount on the physical characterisation is reported in Fig. 6: we observe a constant density associated with a stable electrical conductivity. Concerning the glass transition temperature a small decrease is observed in presence of 4% of Tergitol which plays the role of a plasticizer. In the following part therefore we have prepared a first series of

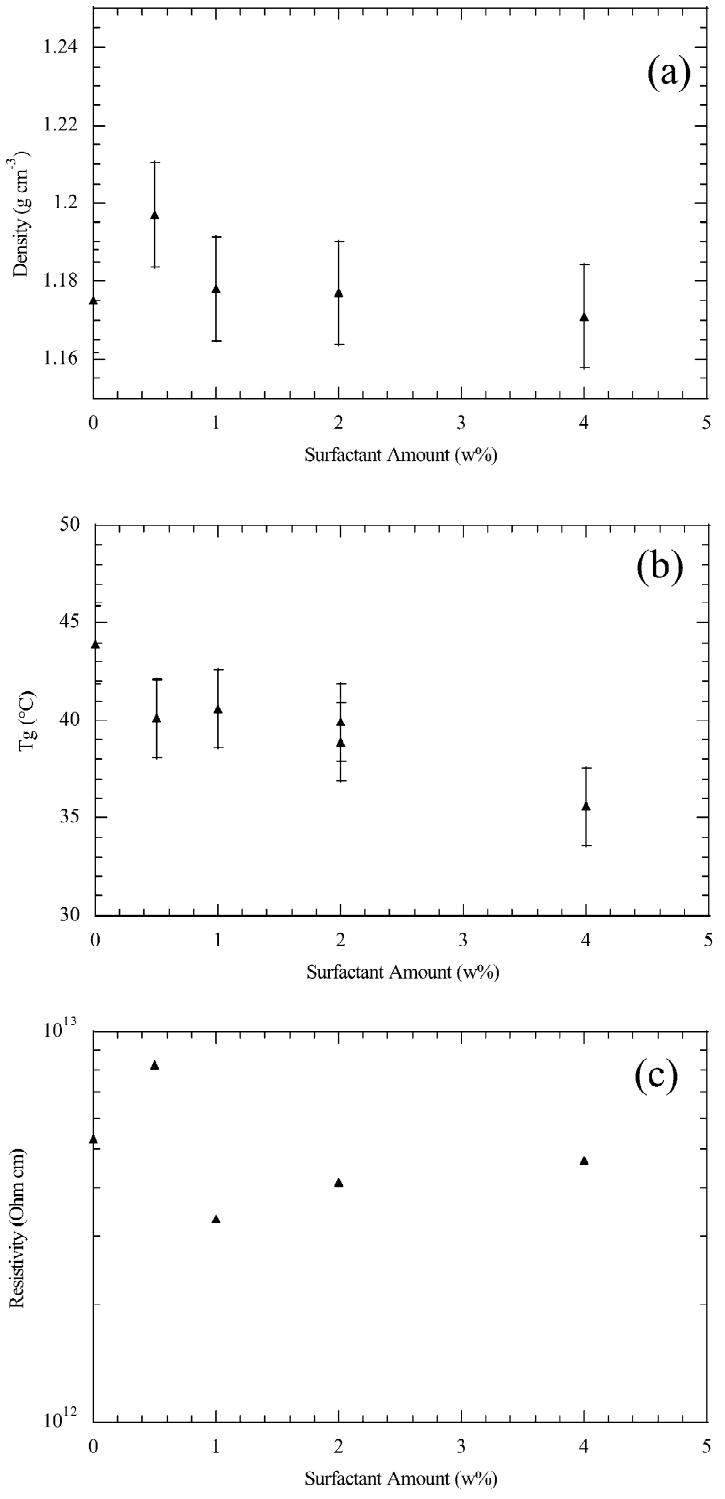

Fig. 6. Physical characteristics: (a) density; (b) glass transition temperature; (c) electrical resistivity of a series of nanocomposites charged with 0.26% in weight of nanotubes and for different surfactant (Tergitol) amounts.

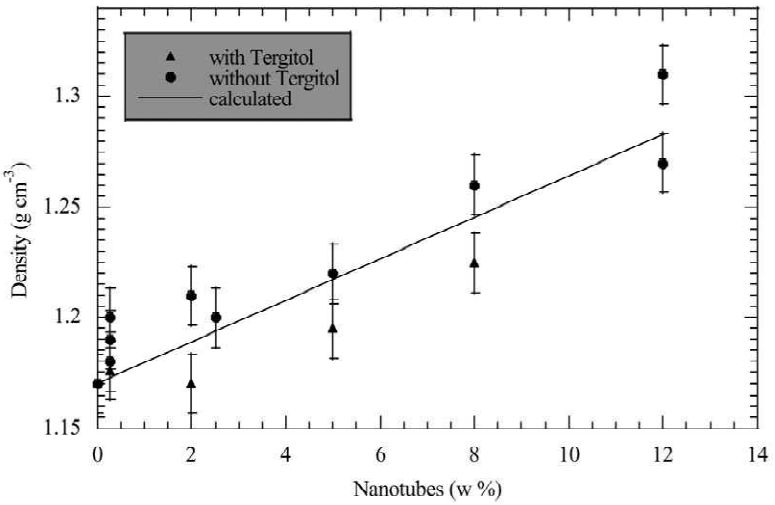

Fig. 7. Nanocomposites density as a function of the nanotubes content for both series of samples.

nanocomposites with different amounts of nanotubes using 2% of Tergitol to be sure that all the carbon surface is covered. For comparison, we also have elaborated a second similar series of samples without any tergitol additive as we will see now.

3.2.2. Influence of nanotube contents

The following two series, in presence of Tergitol or not, have been prepared with different nanotube amounts (batches heat treated or not) changing from 0.26% up to 12% in weight. All the results concerning, respectively, the sample density, the glass transition temperature of the matrix and the electrical resistivity changes are reported in Figs. 7–9. We can examine separately each series of results. For the bulk densities (Fig. 7) we observe for both series an increase with the nanotube content. Concerning the series using the surfactant, it appears that the measured densities are a little lower than for the series without surfactant. It seems to us that in presence of Tergitol, the solvant elimination could be not so completely efficient. A general linear relationship can be drawn as shown in the figure interpolating between the matrix density ($d_m = 1.17$) and a mean nanotube density ($d_{NT} = 2.10$) which is a rather good value in absence of catalyst particles (see Table 1).

Concerning now the glass transition temperature T_g (Fig. 8): its modification with the filler presence is rather smooth as also evidenced with the thermal width values ΔT_g which are always around 30–40 °C. This is in

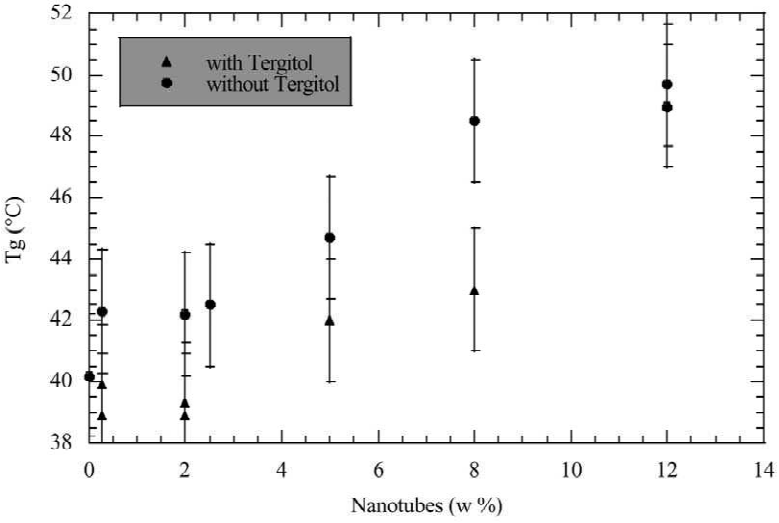

Fig. 8. Direct current electrical resistivity of the nanocomposites versus the nanotubes weight content for both series of samples.

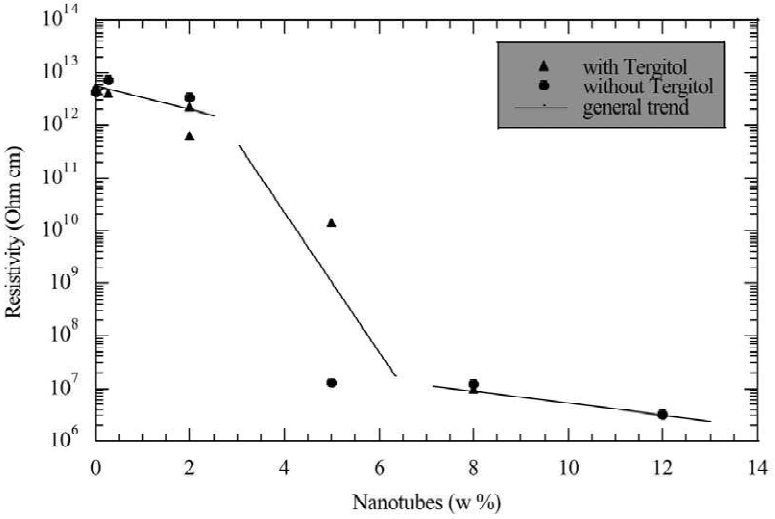

Fig. 9. Glass transition temperature (T_g) versus the nanotubes content for both series of nanocomposites.

contradiction with another study on similar nano-composites using a non ionic surfactant and an epoxy matrix where a rather surprising enhanced T_g value has been found [12]. Nevertheless, for the second series without surfactant, we observe a regular increase of T_g which could be associated with this interfacial behavior. Recently, it has been shown that the glass transition temperature of thin polymer films can be shifted compared to the same bulk polymer [32]. It turns out that an increasing interface area with a rather good anchoring can increase T_g [33]. We assume that it is the current situation which is observed when the Tergitol is not introduced but only the monomer, i.e., when the bisphenol ether is directly wetting the carbon surface. We note finally that for the series prepared with Tergitol no large change of T_g is observed: we presume that there is a competition between the anchoring and the plasticizer effects.

D.c. electrical resistivity (Fig. 9): for the two series a large decrease is observed, around six orders of magnitude, when the nanotube content is reaching about 8% in weight.

These observations are the signature of an observed percolation threshold which corresponds to a critical volumic fraction $\Phi^* \approx 0.04$ as already found for conducting particles with a high geometrical aspect ratio [7,14]. We must notice, however, that these electrical resistivity values, which are isotropic as checked experimentally, appear to reach a plateau which is at a rather higher figure than expected. We know that a compressed pellet of these nanotubes gives a mean resistivity value around 10^{-1} ohm.cm and a smaller limiting value is reached with these nanotubes dispersed in a polystyrene cobutyl acrylate polymer [34]. Besides in presence of this hydrosoluble polymer with latex particles and using SDS as an ionic surfactant a smaller critical volumic fraction has been found ($\Phi^* \approx 0.02$).

To explain this different behavior, it is necessary to imply the interfacial characteristics, assuming therefore that the process leads to a statistical distribution of the nanotubes. Indeed, the wetting of a carbon surface by an aromatic type polymer has been already evidenced with the so-called wrapping effect [35,36]. In our case, as indicated by the increase of the glass transition temperature in presence of bisphenol ether only (Fig. 8), an insulating layer should be wrapped around the nanotubes governing the conduction mechanism as a tunneling effect inside the material. This point is supported by preliminary non-linear current–voltage characteristics observed on the more conducting samples where two defined regions are evidenced (Fig. 10).

These results are in agreement with other reports [37] where a nanocomposite based on a conjugated polymer has evidenced both a relatively high percolation threshold, around 8% in weight of nanotubes, with a similar current–voltage characteristic; the first low field ohmic region is followed by a second one which should imply a different mechanism that we are not able to detail currently.

3.3. Percolation threshold and interfacial properties

The value of the percolation threshold is very sensitive to the polymer type as already shown for carbon particles [14] but also for fibers, nanofilaments and MWNT [34]. For interpreting these results, it is necessary to examine both the interfacial properties between particles and matrix and the processing way. We have, therefore, restricted

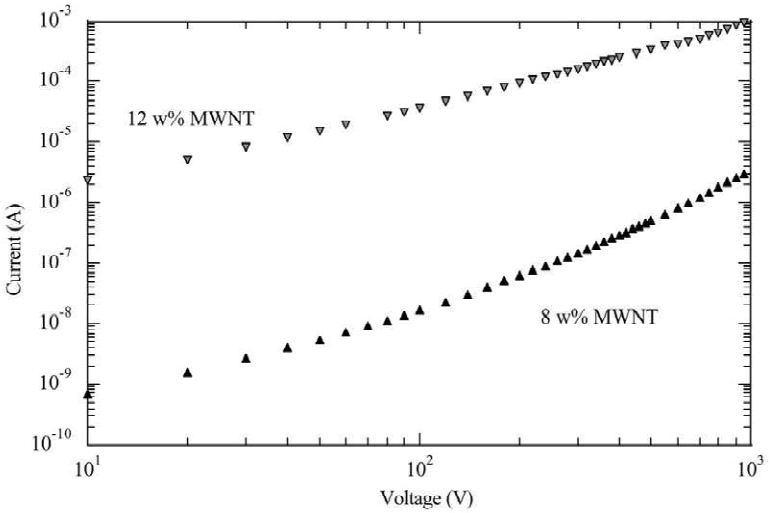

Fig. 10. Logarithmic current–voltage characteristics for 8 and 12% in weight of dispersed nanotubes in the epoxy matrix (without surfactant).

ourselves to the comparison between carbon fillers of different sizes and shapes with the epoxy type matrices. A series of results is summarized in Table 3 where different types of renfort are reported mixed with, more or less, the same series of epoxy resin. We see immediately that the critical volumic fraction is very dependent with the aspect ratio (L/D). This is the first parameter to consider which is ranging between 100 and 1000 for these elongated or disk shape fillers [30,39–41]. The geometrical particle anisotropy with a random distribution inside the matrix is a key factor for determining the percolation threshold. As demonstrated by BALBERG, using a model of excluded volume [42], the critical volumic fraction is proportional to the factor (D^2/L). In the case of statistically distributed

Table 3
Characteristics of different carbon composites prepared with an epoxy resin

Carbon particles As renforts	Geometrical factors (diameter D, length L, thickness e)	Critical volumic fraction (Φ^*)	References
Carbon blacks (Sterling)	Spherical ($D=250$ nm)	0.17	[38]
Carbon blacks (Raven)	Aggregates ($D=30$–50 nm)	0.03–0.10	[39]
Graphite flakes	Disc-shaped $L=10$ μm $e=0.1$ μm	0.013	[40]
Carbon fibers (ex-PAN)	$L=1$–3 mm ($D=10$ μm)	0.005–0.025	[41]
MWNT	$L=1$ μm $D\leq 10$ nm	≈ 0.02	[30]
Nanotubes («fish bone» type)	$L=1$ μm $D=50$ nm	≈ 0.04	This work

rigid and cylindrical rods the calculated critical volumic concentration is estimated between two limits [40]:

$$0.0058 < \Phi^* < 0.0115 \quad (3)$$

It appears, therefore, that the experimental values of Φ^* which are under estimated for MWNT because the nanotubes are hollow, lie outside this range of calculated values based on geometrical parameters only.

It turns out that a second class of parameter is relevant concerning the surface interactions between matrix and particles compared to the particle–particle interactions [7]. Indeed, in presence of a local organization, as the aggregates of small carbon particles, low critical volumic fractions are found [39] as for different type of nanofilaments. Looking for all these values, including our results, we find a range of values spreading on almost one decade which are due to the processing way favorizing the colloidal dispersion thanks to a surfactant but also to the nature of the carbon surface. Indeed, we have demonstrated that the interfacial adhesion with the polymer is good preventing a direct particle–particle interaction and giving rise to a rather high critical volumic fraction for this type of heterogeneous system. This feature should influence also the critical exponent for the electrical conductivity behavior [7] but this is clearly outside the frame of the present study.

4. Conclusion

In this work, we have characterized catalytically vapor grown MWNT by using Raman spectroscopy and diamagnetic susceptibility measurements. We have shown that related to their morphology, these nanotubes are not fully graphitized and their bulk physical properties are controlled by these morphological characteristics, as in other similar carbon materials [43]. Then we have defined a reproducible processing way to prepare two series of nanocomposites with an epoxy resin using, or not, a non-ionic surfactant to disperse the nanofiller. We have shown in particular that in absence of Tergitol used as surfactant, we obtain a valuable dispersion for a stabilized suspension which gives rise to almost the same percolation threshold as deduced from d.c. electrical resistivity measurements (Fig. 9). A more detailed study of the mesostructural organisation would be necessary to understand the details of this phenomenon. It appears nevertheless that the interfacial adhesion between the carbon surface and the polymer is playing a crucial role with the wrapping effect. This is demonstrated by the determination of the glass transition temperature for this thermoset polymer which is depending of the nanotube content. Indeed, in these nanocomposites, the interfacial area, which is inversely proportional to the filler diameter for a given volumic fraction, is higher than for usual composites with fibers. It will play, therefore, a fundamental role for electrical contacts, but also for the mechanical properties through the load transfer between filler and matrix as recently demonstrated [44].

Acknowledgements

The first author, Professor Shen Cui, acknowledges the financial support given by the CNRS (Centre National de la Recherche Scientifique) during his stay at Centre de Recherche Paul Pascal.

References

[1] Delhaes P. Polymorphism of carbon in world of carbon. In: Graphite and precursors, Vol. 1, Gordon and Breach, 2001, pp. 1–24.
[2] Ajayan PM. Nanotubes from carbon. Chem Rev 1999;49:1787–99.
[3] Ebbesen T. Sheets, cones, balls and tubes. In: Setton R, Bernier P, Lefrant S, editors, Carbon molecules and materials, Taylor and Francis, chapter 5, 2002, pp. 179–200.
[4] Tibbetts GG. Carbon fibers produced by pyrolysis of natural gas in stainless steel tubes. Appl Phys Lett 1983;42:666–8.
[5] Speck JS, Endo M, Dresselhaus MS. Structure and intercalation of thin benzene derived carbon fibers. J Cryst Growth 1989;94:834–48.
[6] Baker RTK. Catalytic growth of carbon filaments. Carbon 1989;27:315–23.
[7] Carmona F. La conductivité électrique des polymères chargés avec des particules de carbone. Ann Chim Fr 1987;13:343–5.
[8] Frackowiak E, Beguin F. Carbon materials for the electrochemical storage of energy in capacitors. Carbon 2001;39:937–50.
[9] Vix-Guterl C, Dentzer J, Ehrburger P, Menetrier K, Bonnamy S, Beguin F. Surface properties and microstructure of catalytic multi-walled carbon nanotubes. Carbon 2001;39:318–20.
[10] Ajayan PM, Stephan O, Colliex C, Trauth D. Aligned carbon nanotube arrays formed by cutting a polymer resin–nanotube composite. Science 1994;265:1212–4.
[11] Vigolo B, Penicaud A, Coulon C, Sauder C, Pailler R, Journet C, Bernier P, Poulin P. Macroscopic fibers and ribbons of oriented carbon nanotubes. Science 2000;297:1331–4.
[12] Gong X, Liu J, Baskaran S, Voise RD, Young JS. Surfactant-assisted processing of carbon nanotube–polymer composites. Chem Mater 2000;15:1049–52.
[13] Holzinger M, Vostrowsky O, Hirsh A, Hennrich F, Kappes M, Weiss R, Jellen F. Sidewall functionalization of carbon nanotubes. Angew Chem, Int Ed 2001;40:4002–5.
[14] Miyasaka K, Watanabe K, Jojima E, Aida H, Sunita M, Ishikawa K. Electrical conductivity of carbon–polymer composites as a function of carbon content. J Mater Sci 1982;17:1610–6.
[15] Cui S, Lu CZ, Qiao YL, Cui L. Large scale preparation of

carbon nanotubes by nickel catalyzed decomposition of methane at 600 °C. Carbon 1999;37:2070–3.
[16] Iijima S. Helical microtubules of graphitic carbon. Nature 1991;354:56–8.
[17] Liang Q, Gao LZ, Li Q, Tang SH, Liu BC, Yu ZL. Carbon nanotube growth on Ni-particles prepared in situ by reduction of La_2NiO_4. Carbon 2001;39:897–903.
[18] Bonard J-M, Stora T, Salvetat J-P, Maier F, Stöckli T, Duschl C, Forro L, De Heer WA, Chatelain A. Purification and size selection of carbon nanotubes. Adv Mater 1997;9:827–31.
[19] Chen Q, Dai L, Gao M, Huang S, Nau A. Plasma activation of carbon nanotubes for chemical modification. J Phys Chem B 2001;105:618–22.
[20] Pacault A, Marchand A. Propriétés électroniques des carbones prégraphitiques. J de Chimie Physique 1960;37:873–91.
[21] Chauvet O, Forro L, Bacsa W, Ugarte D, Doudin B, De Heer WA. Magnetic anisotropies of aligned nanotubes. Phys Rev B 1995;52:R6963–6.
[22] Kotosonov AS, Kuvhinnikov SV. Diamagnetism of some quasi two-dimensional graphites and multiwall carbon nanotubes. Phys Lett A 1997;229:377–80.
[23] Dresselhaus MS, Eklund PC. Phonons in carbon nanotubes. Adv Phys 2000;49:705–814.
[24] Lespade P, Marchand A, Couzi M, Cruege F. Caracterisation de materiaux carbones par microspectrometrie Raman. Carbon 1984;22:375–85.
[25] Truinstra F, Koenig JL. Characterization of graphite fiber surfaces with Raman spectroscopy. J Composite Mater 1970;4:492–9.
[26] Matthews MJ, Pimenta MN, Dresselhaus G, Dresselhaus MS, Endo M. Origin of dispersive effects of the Raman *D*-band in carbon materials. Phys Rev B 1999;59:6585–8.
[27] Alvergnat-Gaucher H. Ph. Dissertation: Les nanotubes de carbone catalytiques, Universtité d'Orléans France, 1998.
[28] Endo M, Kin YA, Hayashi T, Nishimura K, Matusita T, Miyashita K, Dresselhaus NS. Vapor grown carbon fibers (VGCF), basic properties and their batteries applications. Carbon 2001;39:1287–97.
[29] Montes-Moran MA, Young RJ. Raman spectroscopy study of HM carbon fibers. Carbon 2002;40:845–55.
[30] Sandler J, Shaffer MSP, Prasse T, Bauhofer W, Schulte K, Windle AH. Development of a dispersion process for carbon nanotubes in an epoxy matrix and the resulting electrical properties. Polymer 1999;40:5967–71.
[31] Lourie O, Wagner HD. Transmission electron microscopy observations of fractures of single wall carbon nanotubes under axial tension. Appl Phys Lett 1998;73:3522–9.
[32] Keddie Jl, Jones RAL, Cory RA. Size dependent depressions of the glass transition temperature in polymer films. Europhys Lett 1994;21:59–64.
[33] Long D, Lequeux F. Heterogeneous dynamics at the glass transition in Van der Waals liquids in the bulk and in thin films. Euro Phys J E 2001;4:371–87.
[34] Dufresne A, Paillet M, Putaux J-L, Canet R, Carmona F, Delhaes P, Cui S. Processing and characterization of carbon nanotube/poly(styrene-cobutyl acrilate) nanocomposites. J Mater Sci 2002;37:3915–23.
[35] Tang BZ, Xu H. Preparation, alignment and optical properties of soluble poly(phenylacetylene) wrapped carbon nanotubes. Macromolecules 1994;32:2569–76.
[36] O'Connel MJ, Boul P, Ericson LN, Huffman C, Wang Y, Haroz E, Kuper C, Tour J, Ausman KD, Smalley RE. Reversible water solubilization of single-walled carbon nanotubes by polymer wrapping. Chem Phys Lett 2001;342:265–71.
[37] Coleman JN, Curran S, Dalton AB, Davey AP, McCarthy B, Blau W, Barklie RC. Percolation dominated conductivity in a conjugated polymer–carbon nanotube composite. Phys Rev B 1998;58:R7492–5.
[38] Fug G, Canet R, Delhaes P. Conductivité électrique de mélanges hétérogènes. C R Acad Sci Paris 1978;2873:5–9.
[39] Salome L, Carmona F. Fractal structure study of carbon blacks used as conducting polymer fillers. Carbon 1991;29:599–604.
[40] Celzard A, McRae E, Deleuze C, Dufort M, Furdin G, Mareche J-F. Critical concentration in percolating systems containing a high aspect ratio filler. Phys Rev B 1996;53:6209–14.
[41] Carmona F, Barreau F, Canet R, Delhaes P. An experimental model for studying the effect of anisotropy on percolative conduction. J Phys Lett 1980;41:531–5.
[42] Balberg I, Binenbaum N, Wagner N. Percolation thresholds in the three dimensional sticks systems. Phys Rev Lett 1984;52:1465–9.
[43] Chung DDL. Comparison of submicron–diameter carbon filaments and conventional carbon fibers as fillers in composite materials. Carbon 2001;39:1119–25.
[44] Lau KT, Hui D. Effectiveness of using carbon nanotubes as nano-reinforcements for advanced composite structures. Carbon 2002;40:1605–6.